Searching for SUSY at the upgraded LHC

CERN Summer Student Program 2013

Sébastien Rettie
University of Ottawa

September 12, 2013

Supervisor:
Dr. Anadi Canepa
TRIUMF

Contents

Abstract

We investigate the pair production of $\tilde{\chi}_1^{\pm}\tilde{\chi}_2^0$ followed by a subsequent decay into the W and the Higgs SM bosons using events with 3 leptons and missing transverse momentum ($E_{\mathrm{T}}^{\mathrm{miss}}$) and the ATLAS detector at the LHC. A cut-and-count analysis is presented with the assumption of 3000fb^{-1} of proton-proton collision data at 14 TeV center-of-mass energy at the LHC. The results are interpreted as discovery and exclusion reaches.

1 Introduction

1.1 Supersymmetry

The standard model (SM) of particle physics is a predictive theory which explains most of the fundamental interactions of elementary particles. However, it is known to be an effective theory in the sense that it is valid only in a given energy range, and that it does not account for many observed experimental results: for example, it does not offer a satisfying explanation for neutrino masses and mixing, or dark matter. From a theoretical point of view, the standard model fails when it comes to explaining the hierarchy problem, the unification of forces, etc. [1]. The minimal supersymmetric standard model (MSSM) offers a solution to many of these problems by introducing superpartners to every SM particle that differ in spin by $1/2$ (see figure 1a); every SM fermion (boson) is associated to a supersymmetric boson (fermion). The naming convention for the supersymmetric partners of the SM particles is to add an "s" (for scalar) in front of SM fermions (which become sfermions) and to add an "ino" at the end of the SM bosons (e.g. gauge bosons become gauginos). Also, all SUSY particles have a tilde ($\sim$) over the symbol representing them.

SUSY predicts that the masses of the SM particles are identical to the masses of their respective superpartners. However, from experimental data, we know that SUSY particles do not have the same mass as their SM partners; there has been no observation of light sparticles such as the selectron of the smuon. Hence, we assume that SUSY is a broken symmetry. The mechanism that breaks this symmetry remains, at the moment, unknown. The model used in this analysis is the minimal supersymmetric standard model (MSSM). In the MSSM, there are two complex Higgs doublets $H_u = (H_u^+, H_u^0)$ and $H_d = (H_d^0, H_d^-)$, which have higgsino superpartners. Because of electroweak symmetry breaking, the charged higgsinos and winos mix to form mass eigenstates called charginos ($\tilde{\chi}_i^{\pm}$, $i = 1, 2$),

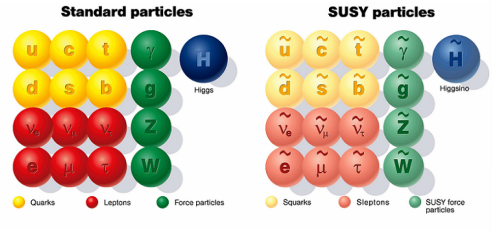

(a) Elementary particles of the SM (left), and their corresponding supersymmetric partners, or sparticles (right).

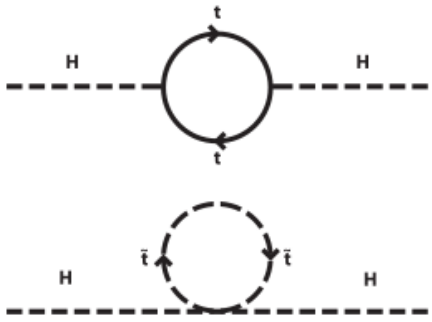

(b) Top and stop quark quantum loop corrections; their contributions cancel out and thus the MSSM offers a solution to the hierarchy problem.

Figure 1: The MSSM and its solution to the hierarchy problem.

while the neutral higgsinos, winos and binos mix to form mass eigenstates called neutralinos ($\tilde{\chi}_j^0$, $j = 1, 2, 3, 4$). SUSY solves the hierarchy problem (i.e. having to tune the Higgs mass up to the 34^{th} digit!) because it introduces the stop quark; the stop quantum loop corrections then cancel the contributions from the top loops, which removes the need of fine tuning when considering the Higgs mass (see figure 1b). Also, the gauge couplings of the electromagnetic, the strong and the weak force all unify at $\sim 10^{16}$ GeV in SUSY. Finally, SUSY can provide an excellent candidate for Dark Matter (DM).

1.2 R-Parity

An important note for this study is that our model respects R-parity. R-parity is a property of a particle defined in equation 1, where B is the baryon number, L is the lepton number, and s is the spin of the particle.

$$P_R = (-1)^{3(B-L)+2s} \tag{1}$$

It is introduced into SUSY to help avoid interactions that could violate the lepton and baryon numbers (e.g. proton decay). Standard model particles have $P_R = 1$, and SUSY particles have $P_R = -1$. Therefore, the number of SUSY particles in a given interaction vertex must always be even if R-Parity is con-

served. If the parity is conserved, SUSY particles are always created in pairs, and a decaying SUSY particle always has a SUSY particle in its decay products. Finally, R-parity implies that the lightest supersymmetric particle (LSP) must be stable (because it cannot decay to a non-SUSY particle state). In a large region of SUSY parameter space, the LSP is the lightest neutralino, thus neutral and weakly interacting. Seeing as the LSP is stable, neutral, and weakly interacting, this is a great Dark matter candidate.

1.3 Searching for SUSY

The ATLAS detector at the LHC has a wide range of ongoing searches looking for SUSY. It has already searched for strongly produced sparticles (e.g. squarks, gluinos, stops, sbottoms) [2] [3] and for weakly produced sparticles (e.g. charginos, neutralinos, sleptons). The most up-to-date results of the ATLAS searches for SUSY can be found at [4]. So far, no excess of events has been found. The LHC is a proton-proton collider that ran up to 8 TeV center-of-mass energy over the past few years, and has collected more than 20 fb^{-1} of data. There is a planned upgrade in 2018 that will bring the center-of-mass energy up to 14 TeV and will allow researchers to collect over 3000 fb^{-1} of data. This corresponds to phase 2 as described in figure 2 (i.e. the HL-LHC).

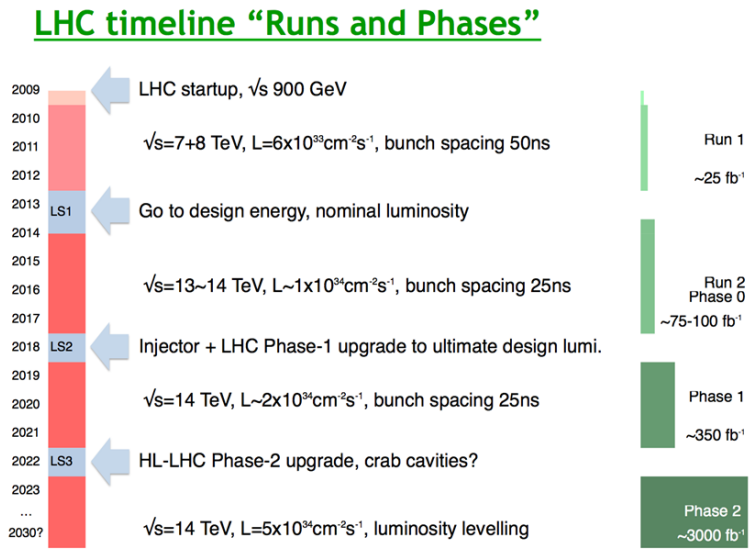

Figure 2: Planned upgrade timeline for the LHC.

2 Signal

The presented study uses the assumption that the high luminosity LHC (HL-LHC) will be able to acquire 3000 fb^{-1} of data with a 14 GeV center-of-mass energy. The focus of this study is centered around searching for weakly produced SUSY. More specifically, we will investigate the pair production of $\tilde{\chi}_1^{\pm}$ and $\tilde{\chi}_2^0$. The particular channel presented in this document is the pair production of a $\tilde{\chi}_1^{\pm}$ and a $\tilde{\chi}_2^0$, with the $\tilde{\chi}_1^{\pm}$ decaying into a W boson and a $\tilde{\chi}_1^0$, and the $\tilde{\chi}_2^0$ decaying into a Higgs boson and a $\tilde{\chi}_1^0$ (see figure 3). The long sought after Higgs boson has a variety of decay modes (i.e. different ways to decay). The probability of these decays occuring (i.e. the branching ratios of the processes) is dependent on the mass of the Higgs boson. Figure 4 shows the different branching ratios for the SM Higgs boson. We know that the mass of the Higgs is around 125 GeV [5]. Hence, we see that the main decay mode for the Higgs is by far $b\bar{b}$ (note the log scale on figure 4). However, the Higgs also decays into WW and ZZ with non-negligible branching ratios. The W boson decays into a lepton and a neutrino with a branching ratio of 32.57%, and the Z boson decays into to leptons with a branching ratio of 10.096% [6][7]. Since leptons are extremely "clean" compared to quarks (i.e. can be well identified and reconstructed in the ATLAS detector), we realize that it is important to search for these processes, despite the minuscule branching ratio of the Higgs decaying into WW (21.5%) or into ZZ (2.64%) [8]. Hence, in the final state, we are left with 3 stable leptons (for this study, only electrons and muons), and missing transverse momentum ($E_{\mathrm{T}}^{\mathrm{miss}}$).

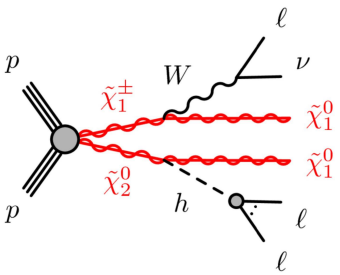

Figure 3: Feynmann diagram of a proton-proton collision at the LHC pair producing a $\tilde{\chi}_1^{\pm}$ and a $\tilde{\chi}_2^0$, which then decay into $W\tilde{\chi}_1^0$ and $h\tilde{\chi}_1^0$, respectively.

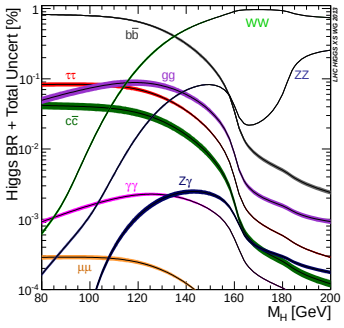

Figure 4: Standard Model Higgs boson decay branching ratios.

3 Backgrounds

There are many SM backgrounds to this signal (i.e. other SM processes with the same signature of 3 leptons and $E_{\mathrm{T}}^{\mathrm{miss}}$). The cross sections of the SM backgrounds vary greatly. Looking at table 1, we see that the dominant background is by far the $t\bar{t}$.

SM Background	σ
WZ (157953)	51.8 pb
WH (161105)	1.504 pb
WWW^* (167006)	143.0 fb
ZWW^* (167007)	182.0 fb
ZZZ^* (167008)	15.0 fb
$t\bar{t}$ (105200)	977.7 pb
$t\bar{t}W$ (119353)	0.25*1.22 pb

Table 1: Cross sections used for SM backgrounds.

Seeing as these SM processes are background processes, there must be a way for them to decay into a final state of 3 leptons and missing transverse momentum. Below is a short description of how they reach this final state.

WZ and WH diboson production In this SM background, the W boson decays into a lepton and a neutrino, and the Z boson or Higgs boson decays into two leptons. Hence in the final state we are left with 3 leptons and a neutrino.

Triboson production This SM background is relatively self-explanatory. Each of the 3 bosons in the process is capable of producing one or more leptons (i.e. the W boson can decay into a lepton and a neutrino, and the Z boson can decay into 2 leptons); ending up with 3 leptons in the final state is then simple.

$t\bar{t}$ **production** The main background for this study has an extremely large cross section compared to the signal cross sections (see table 1). Both top quarks start by decaying into a W boson and a bottom quark. Then, both W bosons decay into a lepton and a neutrino. Finally, one of the bottom quarks decays leptonically to produce 3 leptons in the final state.

$t\bar{t}W$ **production** Similar to the $t\bar{t}$ production, this background gets two leptons from the W bosons coming from the top quarks, with its third lepton coming from the third W boson in the process; it does not need a lepton coming from a bottom quark.

4 Event selection

The ATLAS (A Toroidal LHC ApparatuS) detector is a general-purpose particle physics detector at the LHC. Its cylindrical shape allows for the detection of proton-proton collisions and their decay products in almost all directions. To detect these particles, ATLAS uses tracking detectors, calorimeters, and muon chambers. Of course, ATLAS has certain limitations when it comes to its resolution and its efficiency. For example, the number of collisions occuring per bunch crossing is not a single collision. So, when trying to model background processes, one has to take this into account. One of the main challenges for the HL-LHC will be the manner in which it handles this large number (expected to be on the order of 140) of collisions per bunch crossing; we call this pileup. Also, the ATLAS tracking detector collects the signal produced by charged particles, which are then converted to "tracks" using advanced reconstruction algorithms. Once we have tracks, the properties of this track are examined to try and determine what type of particle the detector actually measured (e.g. a track matched to an electromagnetic cluster is a good electron candidate). Seeing as we do not have any data from the HL-LHC, this study is a so-called "truth-based" study; we only use event generators to get our information. Smearing is then applied to emulate the actual signals we would get in the ATLAS detector. Starting from the truth based n-tuples, each event used in the analysis is required to meet certain criteria to be considered. Once an event has passed the basic event selection, it is then kept for the analysis based on selection criteria. An important quantity considered when selecting events is the pseudorapidity η of an object (e.g. a lepton, or a jet). Pseudorapitidy is a spatial coordinate that describes the angle of a particle with respect to the beam axis. The pseudorapidity is defined by equation 2, where θ is the angle between the particle momentum and the beam axis.

$$\eta = -\ln\left[\tan\left(\frac{\theta}{2}\right)\right] \tag{2}$$

When the two proton beams collide in the ATLAS detector, they do so along a unique axis; let us say the z-axis. We can define a transverse plane as a plane

that has the beam crossing it with a $90°$ incidence angle; in our case, the xy plane. From there, we can define the transverse momentum (p_{T}) of a particle as being the projection of its momentum vector onto this transverse plane.

4.1 Analysis strategy

A priori, we do not know the masses of the $\tilde{\chi}_i^{\pm}$, $i = 1, 2$ or the $\tilde{\chi}_j^0$, $j = 1, 2, 3, 4$. To simplify our search, we assume that the mass of the $\tilde{\chi}_1^{\pm}$ is equal to the mass of the $\tilde{\chi}_2^0$. Hence, we only need to input two parameters into our searches (i.e. the mass of the $\tilde{\chi}_1^{\pm}$ and the mass of the $\tilde{\chi}_1^0$) before we are able to look for SUSY. This is then easily translated to a 2D grid, with the mass of the $\tilde{\chi}_1^{\pm}$ and $\tilde{\chi}_2^0$ on the x-axis, and the mass of the $\tilde{\chi}_1^0$ on the y-axis; the z-axis corresponding to the sensitivity to that particular combination of electro-weakino masses. Of course, the cross sections vary with respect to the different input parameters; figure 5 shows the various cross sections calculated using the program called PROSPINO. Once we identify the processes that have a similar signature to the signals' signature, we define a set of selection criteria to differentiate the signal from the SM backgrounds. We fine-tune these selection criteria by maximizing the Z_n of the distributions (see section 6.3).

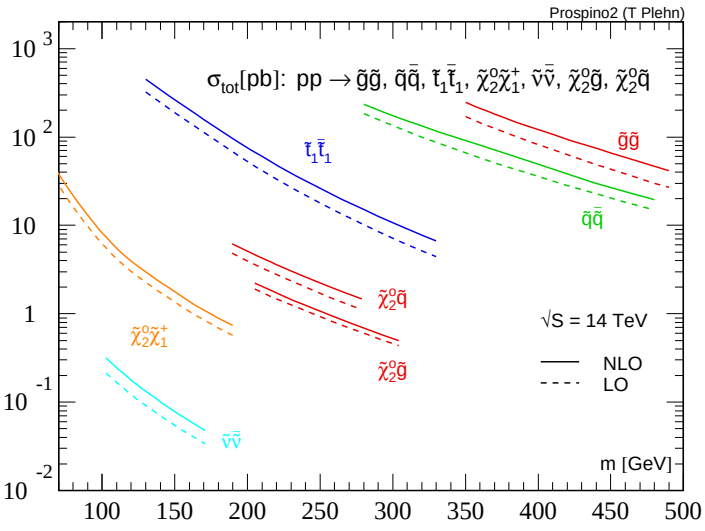

Figure 5: Calculated cross sections depending on the $\tilde{\chi}_1^{\pm}$ and $\tilde{\chi}_1^0$ masses.

4.2 Preselection

Considering each and every object in an event would require far too much CPU time. To concentrate our efforts only on interesting particles, a preselection is first applied:

- Electrons with $p_{\mathrm{T}} > 5$ GeV
- Muons with $p_{\mathrm{T}} > 5$ GeV
- Jets with $p_{\mathrm{T}} > 10$ GeV

4.3 Smearing

After preselection, we use the `TruthToRecoFunctions` RootCore packages to smear the lepton p_{T} and the $E_{\mathrm{T}}^{\mathrm{miss}}$. This is done to simulate as accurately as possible the detector resolution, since we only have truth based event generations, and not reconstructed objects.

4.4 Object definition

The next step is to select leptons and jets that meet the requirements below. Our signal mainly contains electrons and muons with $p_{\mathrm{T}} > 10$ GeV, so there is no need to keep events with lower p_{T} leptons. Note that we do not consider hadronically decaying taus in this study.

- Electrons: $p_{\mathrm{T}} > 10$ GeV and $|\eta| < 2.47$.
- Muon: $p_{\mathrm{T}} > 10$ GeV and $|\eta| < 2.50$.
- Jets: $p_{\mathrm{T}} > 20$ GeV and $|\eta| < 2.50$.

4.5 Overlap removal

A key step in making sure we get a clean signal is to apply a rigorous overlap removal to get rid of any unwanted objects.

- Discard the electron with the lowest E_T if $\Delta R_{ele,ele} < 0.1$. This removes duplicated electrons.

- Discard a jet if $\Delta R_{ele,jet} < 0.2$. This removes duplicate objects across electron and jet containers.
- Discard electron if $\Delta R_{ele,jet} < 0.4$. This removes electrons within remaining jets.
- Discard muon if $\Delta R_{\mu,jet} < 0.4$. This removes muons within remaining jets.
- Discard both electron and muon if $\Delta R_{\mu,ele} < 0.1$. This removes overlapping electrons and muons from bremmstrahlung.

4.6 b-jet tagging

Seeing as the LHC is a proton collider, there is an extremely high probability of producing jets from quarks and/or gluons in a given event. Hence, the ATLAS detector detects a large number of jets per event. One important property of a jet is its flavour (i.e. the flavour of the quark that created the jet in the detector). b-jet tagging (or b-tagging) is an algorithm that tries to determine if the detected jet originated from a b-quark. The algorithm is based on a neural network approach which uses the information that the ATLAS detector can obtain: mass of the jet, number of tracks in the jet, how displaced the decay vertex is with respect to the primary vertex, etc. Figure 5 of [9] shows the efficiency of b-tagging for b-jets, c-jets, and light jets as a function of the jets' η and p_{T}. We see that the efficiency of correctly tagging a b-jet decreases with increasing η. This is due to the fact that the tracker ends at $\eta = 2.5$, and so it is impossible to reconstruct a track with this large of an η. Without a track, one does not have the information regarding the position of the vertex of the jet, the mass of the jet, etc., which makes it extremely difficult to correctly identify a b-jet. Ideally, the b-tagging algorithm should have an efficiency of 100% for jets originating from b-flavoured quarks, and an efficiency of 0% for quarks originating from other quarks. However, since c-quarks have a mass and lifetime close to those of the b-quarks (1.275 GeV for c-quarks and 4.18 GeV for b-quarks [10]), it is possible to mis-identify them in certain instances. Because the other "light flavour" quarks have much smaller lifetimes and masses on the order of a few MeV, it is much easier to differentiate between them and b-quarks, hence the low b-tagging efficiency for "light flavour" quarks. It is important that we implement this b-tagging in our analysis so as to take into account the probability of correctly identifying a b-jet, and hence certain types of events.

4.7 Trigger

It is absolutely impossible for the ATLAS detector to record every single event that passes through it onto tape; doing so would result in writing to disk up to 10^5 petabytes of data per year! For reference, a mere 50 petabytes is roughly the entire written works of mankind, from the beginning of recorded history, in all languages. So, we need a fast, online (i.e. in real time) filter that can make quick decisions on whether or not the event could potentially be interesting for physics analyses; this is the trigger. We define a set of "easy to check" critera that allow us to reject most LHC collisions prior to storage on tape. For this study, these criteria are one of the following.

- Electron: $p_{\mathrm{T}} > 25$ GeV and $|\eta| < 2.47$.
- Muon: $p_{\mathrm{T}} > 25$ GeV and $|\eta| < 2.40$.

5 Observables

To discriminate background events from signal events and gain sensitivity to a certain process, one has to define a set of observables that will behave differently in background and signal processes. Then, one can apply selection criteria to these observables and retain mostly signal events. The main observables used in this analysis are described below.

5.1 Missing transverse momentum ($E_{\mathrm{T}}^{\mathrm{miss}}$)

ATLAS can detect a panoply of different particles. However, it is not capable of detecting neutral, weakly interacting particles which manage to escape ATLAS, for example neutrinos and neutralinos. In our case, we would very much like to detect the LSP that is necessarily stable if R-parity is conserved. We know that when a collision occurs in the ATLAS detector, there is initially no transverse momentum. We can imagine two proton beams propagating along the z-axis; momentum in the transverse xy plane is 0. Hence, by vectorially summing up all the momenta of all the detected particles, one can infer the value of the missing transverse momentum of the event ($E_{\mathrm{T}}^{\mathrm{miss}}$). This $E_{\mathrm{T}}^{\mathrm{miss}}$ is thus the sum of the transverse momenta of the particles escaping the detector without interacting. Equation 3 gives the definition of $E_{\mathrm{T}}^{\mathrm{miss}}$. A more detailed calculation is given in [11]. We can use the $E_{\mathrm{T}}^{\mathrm{miss}}$ to discriminate our signal from our background because the amount

of missing transverse momentum coming from each process should differ depending on what particles can escape our detector. For example, the WZ background process has only one neutrino coming from the W that contributes to the $E_{\mathrm{T}}^{\mathrm{miss}}$. On the other hand, our signal contains one neutrino coming from the W, and two LSPs in the final state.

$$E_{\mathrm{T}}^{\mathrm{miss}} = \sqrt{E_{\mathrm{x}}^{\mathrm{miss}\,2} + E_{\mathrm{y}}^{\mathrm{miss}\,2}} = -\sum_{\text{Objects}} \mathbf{p}_{\mathrm{T}} \tag{3}$$

5.2 Transverse mass (m_{T})

An interesting kinematic variable that is used in this analysis is the transverse mass m_{T}. The analogy used to understand the concept of transverse mass is the invariant mass of the Z boson. We know that the Z boson can decay into two leptons; we can determine the mass of the Z boson from the measured momenta of the leptons using equation 4.

$$M_Z^2 = (E_{l_1} + E_{l_2})^2 - (p_{l_1} + p_{l_2})^2 \tag{4}$$

The same procedure can be applied for the W boson, but instead of 2 leptons, we have a lepton and a neutrino (i.e. we use the momentum of the lepton and the $E_{\mathrm{T}}^{\mathrm{miss}}$ from the neutrino). The m_{T} is the quantity expressed in equation 5, where ϕ is the angle between the $E_{\mathrm{T}}^{\mathrm{miss}}$ and the transverse momentum of the lepton being used for the m_{T} calculation. A more detailed explanation of the transverse mass can be found in [12]. The transverse mass was first introduced to calculate the mass of the W boson. Roughly speaking, the mass of the W boson cannot be measured directly because of the neutrino it decays into (that cannot be directly detected by the ATLAS detector) along with the lepton. However, we know that its mass will be lower than the m_{T}. So, for the WZ background, the m_{T} distribution for the lepton coming from the W should have a Jacobian edge with a rapid drop in the number of events with m_{T} above the W boson mass. The signal should not have such a sharp drop; this is due to the fact that the $E_{\mathrm{T}}^{\mathrm{miss}}$ used for the m_{T} calculation has an extra contribution, the contribution from the $\tilde{\chi}_1^0$.

$$m_{\mathrm{T}} = \sqrt{2 * p_{\mathrm{T}}^{l} * E_{\mathrm{T}}^{\mathrm{miss}}(1 - \cos\phi)} \tag{5}$$

6 Signal regions

In this study we define two signal regions. The first signal region optimization has a same flavour opposite sign (SFOS) lepton pair veto. This signal region focuses mainly on the selection criteria optimization for low $\tilde{\chi}_1^{\pm}\tilde{\chi}_2^0$ mass points. The second signal region optimization does not have the SFOS veto applied, and focuses on optimizing the selection criteria for higher $\tilde{\chi}_1^{\pm}\tilde{\chi}_2^0$ mass points.

6.1 Common selection criteria

The signal region optimizations have a set of basic selection criteria that are common to both of them. These selection criteria are listed below.

3L Select events with 3 leptons in the final state. This is the decay signature we are looking for.

b-Jet Veto The 3 leptons in our signal should be coming from W or Z bosons. Assuming these bosons decay fully leptonically, there should not be any b-quarks in the signals' signature. So if there is a b-jet in the event, this event is most likely a background event.

$\Delta\phi_{min} < 1.0$ Two out of the 3 leptons of our signal are expected to come from the decay of a Higgs boson. If this is the case, these two leptons should be well collimated in the ATLAS detector, and hence have a small $\Delta\phi$. The two leptons should be well collimated mainly because the Higgs has spin-0.

Isolation In this study, we assume that at the time of the HL-LHC, a lepton isolation algorithm with efficiency comparable to the one currently used in the 8 TeV analysis will be available. So, to account for lepton isolation, we multiply the weight of the $t\bar{t}$ sample by a factor of 0.2, which is the efficiency of the isolation requirement as measured in the 8 TeV data.

6.2 Optimization

The optimization for the signal region selection criteria was done in two ways. First of all, we sequentially go through all the selection criteria, one by one, and before each selection criterion, look if the next selection criterion is optimal. Second, we use what are called the "N-1" plots. These are plots of a certain variable

in which all selection criteria are applied except the selection criteria on the variable being plotted. This is done to make sure that all selection criteria are at their optimal value and helps take into account correlations between the selection criteria themselves. Figure 6 show an example of an N-1 plot. All N-1 plots for both signal region optimizations can be found in the appendix of this document.

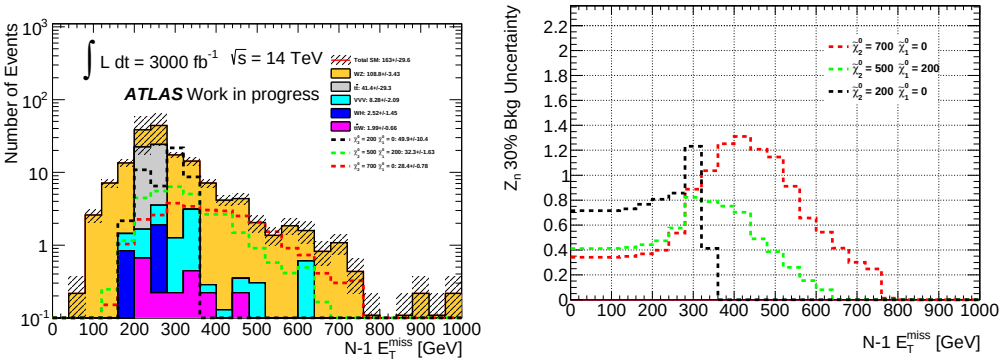

(a) N-1 plot of the $E_{\mathrm{T}}^{\mathrm{miss}}$ for the large electro-weakino mass signal region optimization.

(b) Significance for the N-1 plot of the $E_{\mathrm{T}}^{\mathrm{miss}}$ for the large electro-weakino mass signal region optimization.

Figure 6: Example of an N-1 plot for the large electro-weakino mass signal region optimization.

6.3 Significance (Z_n)

The way to go about searching for SUSY is by trying to detect an excess of events passing certain requirements (i.e. selection criteria) when comparing data to background predictions. If no excess is found, as is currently the case, then one can set limits on the mass of the SUSY particles. The significance Z_n is a value calculated for each combination of the $\tilde{\chi}_1^{\pm} = \tilde{\chi}_2^0, \tilde{\chi}_1^0$ masses. It is roughly equal to the number of signal events divided by the square root of the number of background events left after all of our selection criteria have been applied. However, we use a more complex calculation which takes into account effects such as systematic uncertainties, etc., to which we specify a systematic uncertainty of 30%. If the Z_n value is greater than 1.645, we can exclude the existence of the $\tilde{\chi}_1^{\pm}\tilde{\chi}_2^0$ at the HL-LHC, assuming we collect the 3000 fb^{-1} of data; the given mass scenario is excluded at 95% CL. If the Z_n value is greater than 3, we expect evidence for the

given mass scenario. Finally, if the Z_n value is greater than 5, we expect discovery for the given mass scenario.

6.4 Signal region optimization for low mass electro-weakinos

The number of background and signal events at each stage of the analysis for this signal region can be found in table 2 of the appendix.

SFOS veto For the time being, we focus on the $h \to WW$ decay process. Hence, we require exactly 3 leptons in our final state; considering the $h \to ZZ$ would give us more than 3 leptons in the final state. If an event has a pair of leptons with the same flavour and opposite sign, the pair most likely came from the decay of the Z boson. Since our signal should not contain any Z bosons, the probability for a SFOS pair is lower, and we can veto these events.

$E_{\mathbf{T}}^{\mathbf{miss}} > 100$ **GeV**

Transverse mass selection criteria We apply selection criteria on the transverse mass m_{T} calculated with each of the 3 signal lepton.

- $m_{\mathrm{T}}^1 > 150$ GeV
- $m_{\mathrm{T}}^2 > 150$ GeV
- $m_{\mathrm{T}}^3 > 200$ GeV

6.5 Signal region optimization for large mass electro-weakinos

The number of background and signal events at each stage of the analysis for this signal region can be found in table 3 of the appendix.

Z candidate veto Veto events having a pair of leptons with a mass within 10 GeV of the Z boson mass. Possible lepton pairs are two electrons (regardless or their charge), or two muons with opposite charge.

Low mass off-mass-shell Z veto Veto events having a pair of leptons with a mass smaller than 15 GeV. Possible lepton pairs are two electrons (regardless or their charge), or two muons with opposite charge.

$E_{\mathbf{T}}^{\mathbf{miss}} > 380$ **GeV**

Transverse mass selection criteria We apply selection criteria on the transverse mass m_{T} calculated with each of the 3 signal lepton.

- $m_{\mathrm{T}}^1 > 300$ GeV
- $m_{\mathrm{T}}^2 > 200$ GeV
- $m_{\mathrm{T}}^3 > 150$ GeV

Figure 7 shows the sensitivity obtained for both signal region optimizations. The x-axis is the input mass of the $\tilde{\chi}_1^{\pm}$, which is equal to the mass of the $\tilde{\chi}_2^0$. The y-axis is the mass of the $\tilde{\chi}_1^0$. The z-axis is the sensitivity. The black line in the plot is the "exclusion" line. We see that the low electro-weakino mass optimization is sensitive to a smaller portion of the grid, but get much higher Z_n values for the points which it is sensitive to (able to exclude up to about 550 GeV). On the other hand, the large electro-weakino mass optimization has lower Z_n values in general, but covers much more of the 2D grid.

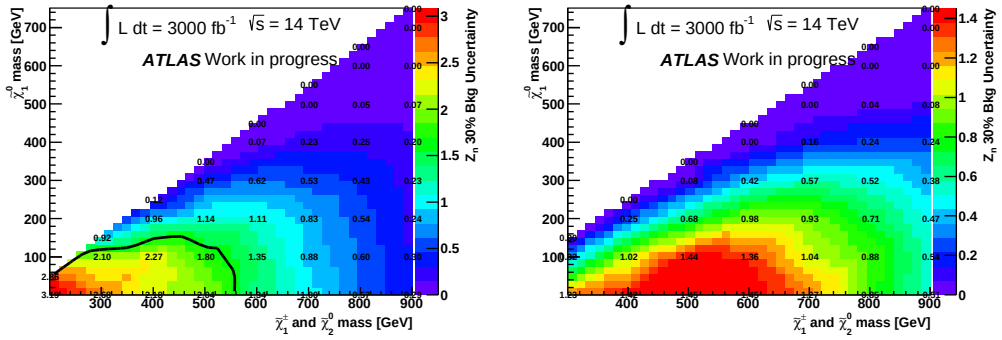

(a) Sensitivity obtained in the low electro-weakino mass signal region optimization.

(b) Sensitivity obtained in the large electro-weakino mass signal region optimization.

Figure 7: Sensitivity for both signal regions with exclusion limits being represented by the black line.

7 Conclusion

We investigated the pair production of $\tilde{\chi}_1^{\pm}\tilde{\chi}_2^0$ with a final state of 3 leptons and missing transverse momentum $E_{\mathrm{T}}^{\mathrm{miss}}$ at the HL-LHC with the assumption of 3000 fb^{-1} of accumulated data and 14 TeV center-of-mass energy. We achieved 3 sigma for the 200 GeV $\tilde{\chi}_1^{\pm}\tilde{\chi}_2^0$ mass point and excluded masses below 550 GeV if the $\tilde{\chi}_1^0$ is massless.

8 Acknowledgements

My work with the ATLAS collaboration has been an excellent learning experience. I would like to sincerely thank my supervisor Dr. Anadi Canepa for her invaluable advice and perpetual help throughout this entire project. I am also thankful to Dr. Zoltan Gecse and Matthew Gignac for their time and effort in answering my questions. I would also like to thank Dr. William Trischuk and the IPP for giving me the opportunity to be part of this CERN summer student program.

Appendices

SR0 Cut Flow and N-1 Plots

Sample	3L	SFOS Veto	Z Candidate Veto	OMS Z Veto	B-jet Veto	MET Cut	dPhiMin Cut	Total Charge Cut	Lepton 1 mT Cut	Lepton 2 mT Cut	Lepton 3 mT Cut
WH	4507.4±61.5	1117.2±30.6	1117.2±30.6	1117.2±30.6	1111.3±30.5	620.3±22.8	454.9±19.5	276.1±15.2	151.9±11.3	36.9±5.57	3.36±1.68
$t\bar{t}W$	10740.2±48.8	3509.7±27.9	3509.7±27.9	3509.7±27.9	1439.8±17.9	921.7±14.3	652.7±12	161.3±5.98	75.3±4.09	23.5±2.28	1.33±0.54
VVV	13942.7±106.2	2902.3±51.3	2902.3±51.3	2902.3±51.3	2891.5±51.2	1715.3±39.6	721.5±25.6	478.2±21.1	301.6±16.8	96.1±9.51	3.96±1.98
WZ	498476.8±232.4	3115.4±18.4	3115.4±18.4	3115.4±18.4	3052.4±18.2	1953.9±14.5	1218.9±11.5	556.2±7.76	197.6±4.63	30.4±1.82	0.87±0.31
$t\bar{t}$	3267656±8227.4	876838.1±4261.9	876838.1±4261.9	876838.1±4261.9	450951.8±3056.4	270894.2±2368.9	176494.5±1912.1	59204.4±1107.4	23014.7±690.5	3604.5±273.3	
Total SM	3795323±8231.8	887482.8±4262.5	887482.8±4262.5	887482.8±4262.5	459446.8±3057.1	276105.6±2369.4	179542.6±1912.4	60676.2±1107.8	23741.2±690.8	3791.4±273.5	9.52±2.67
$\tilde{\chi}_2^0 = 700\tilde{\chi}_1^0 = 0$	141.5±1.75	32.3±0.83	32.3±0.83	32.3±0.83	32.2±0.83	29.1±0.79	26.5±0.76	24.2±0.72	22.4±0.7	16±0.59	5.65±0.35
$\tilde{\chi}_2^0 = 500\tilde{\chi}_1^0 = 200$	543.8±6.7	121.4±3.16	121.4±3.16	121.4±3.16	120.6±3.16	97.2±2.83	80±2.57	73±2.45	61.2±2.25	35.5±1.71	6.44±0.73
$\tilde{\chi}_2^0 = 200\tilde{\chi}_1^0 = 0$	13983.1±174.1	3065±81.5	3065±81.5	3065±81.5	3047.6±81.3	1983.3±65.6	1374.3±54.6	1311.4±53.3	888.7±43.9	312.1±26	19.5±6.5

Table 2: Cut flow table for SR0.

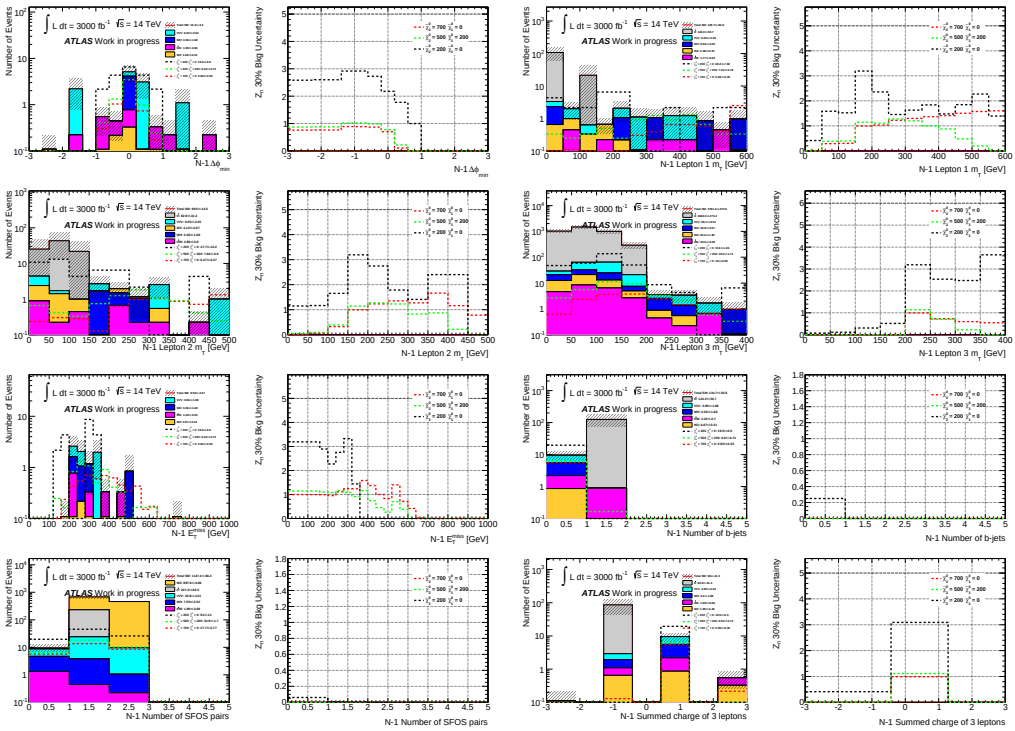

SR1 Cut Flow and N-1 Plots

Sample	3L	SFOS Veto	Z Candidate Veto	OMS Z Veto	B-jet Veto	MET Cut	dPhiMin Cut	Total Charge Cut	Lepton 1 mT Cut	Lepton 2 mT Cut	Lepton 3 mT Cut
WH	4507.4±61.5	4507.4±61.5	4068.4±58.4	3691.5±55.7	3678.9±55.6	14.3±3.46	11.8±3.14	7.55±2.52	4.2±1.88	0.84±0.84	
$t\bar{t}W$	10740.2±48.8	10740.2±48.8	9285.6±45.4	8706.6±43.9	3412.2±27.5	40.3±2.99	25.7±2.39	8.86±1.4	1.77±0.63	0.66±0.38	0.22±0.22
VVV	13942.7±106.2	13942.7±106.2	10668.7±96.2	10176.5±94.7	10139.6±94.6	36.9±5.36	15.5±3.38	10.4±2.8	8.81±2.58	5.17±1.88	1.29±0.55
WZ	498476.8±232.4	498476.8±232.4	134496.1±120.7	69673.1±86.9	68750.6±86.3	844.1±9.56	617±8.17	427.1±6.8	222.8±4.91	121.7±3.63	20.1±1.48
$t\bar{t}$	3267656±8227.4	3267656±8227.4	2851692±7685.9	2612057±7355.9	1299555±5188.5	5717.4±344.1	3956.6±286.3	2175.1±212.3	580±109.6	82.9±41.4	
Total SM	3795323±8231.8	3795323±8231.8	3010211±7687.8	2704305±7357.4	1385536±5190.5	6653±344.4	4626.6±286.5	2629±212.4	817.6±109.8	211.3±41.6	21.7±1.59
$\tilde{\chi}_2^0 = 700\tilde{\chi}_1^0 = 0$	141.5±1.75	141.5±1.75	122.9±1.63	113.1±1.56	112.6±1.56	27.1±0.76	24.9±0.73	23.1±0.71	20.9±0.67	16.7±0.6	13.4±0.54
$\tilde{\chi}_2^0 = 500\tilde{\chi}_1^0 = 200$	543.8±6.7	543.8±6.7	455.5±6.13	421.4±5.9	419±5.88	32.2±1.63	25.9±1.46	24±1.41	18.6±1.24	11.6±0.98	7.59±0.79
$\tilde{\chi}_2^0 = 200\tilde{\chi}_1^0 = 0$	13983.1±174.1	13983.1±174.1	11451.4±157.5	10543.2±151.2	10473.8±150.7	91±14	75.9±12.8	71.5±12.5	41.2±9.45	15.2±5.73	

Table 3: Cut flow table for SR1.

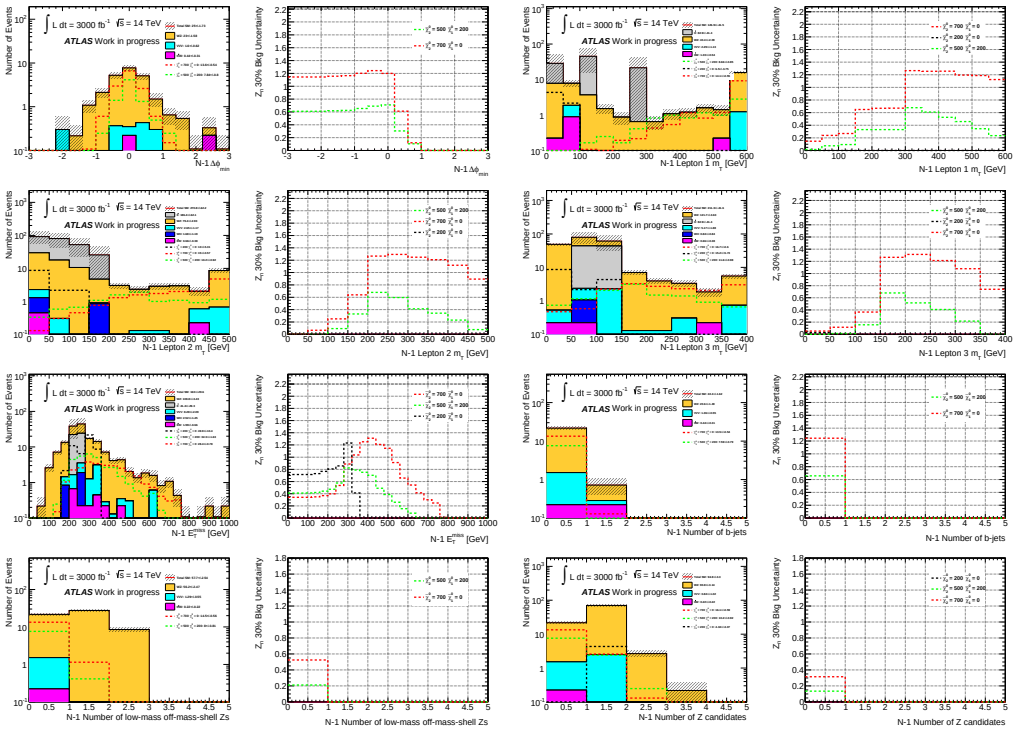

List of Figures

References

[1] A. Masiero, "Highlights on susy phenomenology," *AIP Conference Proceedings*, vol. 744, no. 1, pp. 27–43, 2004.

[2] "Search for direct top squark pair production in final states with one isolated lepton, jets, and missing transverse momentum in $sqrts = 8$,tev pp collisions using 21 fb^{-1} of atlas data," Tech. Rep. ATLAS-CONF-2013-037, CERN, Geneva, Mar 2013.

[3] "Search for squarks and gluinos with the atlas detector using final states with jets and missing transverse momentum and 5.8 fb^{-1} of $\sqrt{s}$=8 tev proton-proton collision data," Tech. Rep. ATLAS-CONF-2012-109, CERN, Geneva, Aug 2012.

[4] `https://twiki.cern.ch/twiki/bin/view/AtlasPublic/SupersymmetryPublicResults`.

[5] "Combined measurements of the mass and signal strength of the higgs-like boson with the atlas detector using up to 25 fb^{-1} of proton-proton collision data," Tech. Rep. ATLAS-CONF-2013-014, CERN, Geneva, Mar 2013.

[6] `http://pdg.lbl.gov/2012/listings/rpp2012-list-w-boson.pdf`.

[7] http://pdg.lbl.gov/2011/listings/rpp2011-list-z-boson.pdf.

[8] https://twiki.cern.ch/twiki/bin/view/LHCPhysics/CERNYellowReportPageBR2.

[9] C. ATLAS, A. Barr, L. Barak, D. Cavalli, M. Duehrssen, F. Filthaut, O. Kortner, E. Lipeles, F. Monticelli, E. Moyse, A. Nisati, F. Parodi, S. Sacerdoti, A. Schwartzman, S. Strandberg, P. Wells, and S. Xella, "Performance assumptions for an upgraded atlas detector at a high-luminosity lhc," Tech. Rep. ATL-PHYS-PUB-2013-004, CERN, Geneva, Mar 2013.

[10] http://pdg.lbl.gov/2012/tables/rpp2012-sum-quarks.pdf.

[11] L. Ancu, A. Canepa, A. De Santo, S. Farrell, C. Gay, Z. Gesce, M. Gignac, S. Haug, O. Jinnouchi, L. Marti, R. Nagai, A. Mete, C. Potter, P. Salvatore, I. Santoyo Castillo, B. Schneider, A. Taffard, and M. Weber, "Search for supersymmetry in events with three leptons and missing transverse momentum in 20.3 fb^{-1} pp collisions at $\sqrt{s}$=8tev with the atlas detector," Tech. Rep. ATL-COM-PHYS-2013-888, CERN, Geneva, Jul 2013.

[12] A. J. Barr and C. G. Lester, "A review of the mass measurement techniques proposed for the large hadron collider," *Journal of Physics G: Nuclear and Particle Physics*, vol. 37, no. 12, p. 123001, 2010.